

# Imidazole-Ligated Compound I Intermediates: The Effects of Hydrogen Bonding

Michael T. Green

Contribution from the Beckman Institute, California Institute of Technology, Pasadena, California 91125

Received December 15, 1999

**Abstract:** An unresolved issue of peroxidase activity is the role played by the hydrogen bond between the proximal histidine ligand and a highly conserved aspartate group. It has been postulated that this hydrogen bond imparts imidazolite character to the axial ligand, increasing its donating ability and stabilizing the high valent compound I intermediate. A general feature of biological compound I intermediates is that they display weaker spin couplings than model systems. To understand how the Asp-His hydrogen bond affects the electronic structure of the compound I intermediate and to establish a connection between it and the decreased coupling strengths observed in peroxidases, we have performed density functional calculations on imidazole- and imidazolite-ligated perferyl porphyrin species. It was found that the imidazolite compound I intermediate possesses an imidazolite-based radical, while the imidazole compound I intermediate possesses a porphyrin-based radical. Delocalization of the radical onto the axial ligand was found to reduce the strength of the spin coupling.

## Introduction

Heme peroxidases are metabolic enzymes that perform a number of biologically important substrate oxidations. The peroxidase active site contains a histidine-ligated iron porphyrin, which reacts with  $\text{H}_2\text{O}_2$  to generate the reactive intermediate compound I. Although these intermediates are thought to be best formulated as ferryl porphyrin radical cations, there has been some indication that the radical species may reside, at least in part, on the axial ligand.<sup>1,2</sup>

One of many unresolved issues concerning peroxidase activity is the role of the hydrogen bond between the proximal histidine ligand and a highly conserved aspartate group. It has been postulated that this hydrogen bond imparts imidazolite character to the histidine ligand, increasing its donating ability and stabilizing the high-valent compound I intermediate.<sup>3</sup>

In a recent communication,<sup>4</sup> the author reported that density functional calculations suggest a strongly donating thiolate ligand (such as that found in nitric oxide synthase, chloroperoxidase (CPO), and cytochrome P450) can alter the electronic structure of the compound I intermediate. Our study revealed that in these systems it is the thiolate ligand, not the porphyrin, that is preferentially oxidized to generate the radical species.

Based upon the results obtained for thiolate-ligated systems, one might expect that the increased donating ability, generated by the Asp-His hydrogen bond of peroxidases, could result in compound I intermediates with histidine-based radicals. This conclusion, which is in contrast to current opinion, appears to be supported by the NMR experiments of La Mar and co-workers.<sup>1</sup> These researchers found that one of the most strongly contact-shifted resonances of horseradish peroxidase compound

I (HRP-I) could not be assigned to the porphyrin, indicating that the radical must be delocalized to some amino acid residue. By studying the relaxation properties of the non-heme contact-shifted signal, they were able to identify this residue as the axial histidine ligand.

A notable difference between the compound I intermediates of peroxidases and the model complexes which seek to mimic them is the strength of the spin coupling between the  $S = 1$  iron-oxo unit and the  $S = 1/2$  radical. Irrespective of their symmetry or axial ligation, model complexes generally display strong ferromagnetic coupling with  $J$  values ranging between 25 and 60  $\text{cm}^{-1}$ ,<sup>5–9</sup> while the coupling in peroxidases is somewhat weaker,  $J = 0–10 \text{ cm}^{-1}$ .<sup>10–12</sup> The data for horseradish peroxidase compound I is in fact best fit with a distribution of weak ferromagnetic and antiferromagnetic interactions ( $|J| \leq 2 \text{ cm}^{-1}$ ).<sup>10</sup>

An important result from our investigation of thiolate-ligated systems is that the antiferromagnetic coupling observed in CPO-I ( $J = -35 \text{ cm}^{-1}$ )<sup>13</sup> can be understood in terms of a weak  $\pi$  interaction between the sulfur-based radical and a member of the  $\text{FeO } \pi^*$  set.<sup>4</sup> In light of this result and the experimental findings of La Mar and co-workers, it seems likely that a similar

(5) Bosso, B.; Lang, G.; McMurry, T. J.; Groves, J. T. *J. Chem. Phys.* **1983**, *79*, 1122–1126.

(6) Mandon, D.; Weiss, R.; Jayaraj, K.; Gold, A.; Terner, J.; Bill, E.; Trautwein, A. X. *Inorg. Chem.* **1992**, *31*, 4404–4409.

(7) Paulsen, H.; Muther, M.; Grodzicki, M.; Trautwein, A. X.; Bill, E. *Bull. Soc. Chim. Fr.* **1996**, *133*, 703–710.

(8) Fujii, H.; Yoshimura, T.; Kamada, H. *Inorg. Chem.* **1996**, *35*, 2373–2377.

(9) Weiss, R.; Mandon, D.; Wolter, T.; Trautwein, A. X.; Muther, M.; Bill, E.; Gold, A.; Jayaraj, K.; Terner, J. *J. Biol. Inorg. Chem.* **1996**, *1*, 377–383.

(10) Schulz, C. E.; Rutter, R.; Sage, J. T.; Debrunner, P.; Hager, L. P. *Biochemistry* **1984**, *23*, 4743–4754.

(11) Khindaria, A.; Aust, S. D. *Biochemistry* **1996**, *35*, 13107–13111.

(12) Patterson, W. R.; Poulos, T. L.; Goodin, D. B. *Biochemistry* **1995**, *34*, 4342–4345.

(13) Rutter, R.; Hager, L. P.; Dhonau, H.; Hendrich, H.; Valentine, M.; Debrunner, P. *Biochemistry* **1984**, *23*, 6809–6816.

(14) Reference deleted in press.

(1) Thanabal, V.; La Mar, G. N.; de Ropp, J. S. *Biochemistry* **1988**, *27*, 5400–5407.

(2) Deeth, R. J. *J. Am. Chem. Soc.* **1999**, *121*, 6074–6075.

(3) Gajhede, M.; Schuller, D. J.; Henriksen, A.; Smith, A. T.; Poulos, T. L. *Nat. Struct. Biol.* **1997**, *4*, 1032–1038.

(4) Green, M. T. *J. Am. Chem. Soc.* **1999**, *121*, 7939–7940.

**Table 1.** Ground State, Coupling Constant, Bond Distances, and NO (SCF) Spin Densities of Compound I Species

species <sup>c</sup>	ground state	$J$ , cm <sup>-1</sup>	distance			spin density <sup>a,b</sup>			average spin density <sup>a,b</sup>			
			Fe-L	Fe-O	Fe-N <sub>avg</sub>	L	Por	FeO	N	C <sub>m</sub>	C <sub>α</sub>	C <sub>β</sub>
imidazole I	$S = 3/2$	99	2.13	1.65	2.03	0.03 (0.01)	1.02 (0.91)	1.95 (2.08)	0.088 (0.156)	0.151 (0.319)	0.003 (-0.112)	0.005 (-0.005)
imidazolate I	$S = 3/2$	60	2.11	1.66	2.03	0.62 (0.60)	0.43 (0.30)	1.95 (2.10)	0.042 (0.065)	0.057 (0.125)	0.002 (-0.050)	0.002 (-0.004)
thiolate I	$S = 1/2$	-38	2.79	1.65	2.02	-0.81 (-0.82)	-0.13 (-0.27)	1.94 (2.09)	-0.013 (-0.049)	-0.020 (-0.048)	0.002 (0.014)	0.000 (0.000)
imidazolate I*	$S = 3/2$	15	2.19	1.63	2.02	0.81 (0.79)	0.24 (0.15)	1.95 (2.06)	0.023 (0.026)	0.026 (0.052)	0.002 (-0.018)	0.002 (-0.002)
thiolate I*	$S = 1/2$	-59	2.69	1.65	2.02	-0.76 (-0.81)	-0.18 (-0.34)	1.94 (2.15)	-0.020 (-0.069)	-0.024 (-0.057)	0.000 (0.019)	0.000 (0.000)

<sup>a</sup> NO (SCF) spin densities. <sup>b</sup> The NO spin densities shown for the thiolate intermediate are actually natural magnetic orbital (NMO) spin densities. See ref 4. <sup>c</sup> The unstarred results in the top section of the table were obtained by performing geometry optimizations at the B3LYP/6-311G level. The starred results in the bottom section of the table were obtained by performing geometry optimizations with larger basis sets. In particular, the imidazolate I\* results were obtained at the 6-311+G(d) level and the thiolate I\* results were obtained at the 6-311+G level. Diffuse functions were not included on carbon.

interaction could be responsible for the decreased  $J$  values found in peroxidases.

A limited number of theoretical investigations have touched upon the important issue of the Asp-His hydrogen bond. In two cases, calculations were performed on imidazolate-ligated perferryl porphyrin species. One of these studies predicts a ground state without ligand spin density,<sup>15</sup> while the other predicts an imidazolate spin density of 0.21.<sup>2</sup> Other studies have focused on active-site models of cytochrome *c* and ascorbate peroxidases (CCP and APX).<sup>16,17</sup> The active-site models examined contained functional groups from the proximal His-Asp-Trp triad. Both investigations found the proximal tryptophan could be oxidized during compound I formation, but one found oxidation was dependent upon the tryptophan's protonation state.<sup>16</sup> This tryptophan seems to only play a role in CCP-I formation,<sup>12</sup> and it is not present in HRP,<sup>3</sup> lignin peroxidase (LIP),<sup>18</sup> peanut peroxidase (PNP),<sup>19</sup> or arthromyces ramosus peroxidase (ARP).<sup>20</sup> In none of the previous investigations was a  $J$  value determined. Thus, the role of the Asp-His hydrogen bond plays in determining the spin couplings of compound I intermediates remains to be established.

To investigate the possibility that the Asp-His hydrogen bond of peroxidases results in proximal ligands with radical character and that this in turn is responsible for the decreased  $J$  values found in biological systems, we have performed density functional calculations on imidazole- and imidazolate-ligated perferryl porphyrins. These complexes represent the extremes of hydrogen bonding, and as such, their  $J$  values and spin densities should be considered limiting, with the values expected for reasonable forms of hydrogen bonding falling between them. Although many calculations have been performed on compound I type molecules, these are the first which specifically calculate  $J$  values as a function of the axial ligand.

The calculations reported here were performed using the B3LYP hybrid functional.<sup>21,22</sup> This functional includes true Hartree-Fock exchange and gradient corrections that make it superior to the local density and semiempirical methods used previously.<sup>23</sup> The calculations were also performed with diffuse basis functions. These functions are important for describing anionic molecules (like the imidazolate ligand) correctly.<sup>24,25</sup> Importantly, the functional and basis sets employed in these calculations are the same as those used to investigate the thiolate system, allowing the findings of these two studies to be combined. Together they should provide a coherent and encompassing view of the electronic structure of compound I, furthering our understanding of this important intermediate.

## Computational Methods

Using GAUSSIAN94,<sup>22</sup> unrestricted calculations were performed on a 47 (46) atom active-site model of a peroxidase compound I intermediate. The histidine axial-ligand was replaced with an imidazole (imidazolate), and a porphine was substituted for the protoporphyrin unit. Geometry optimization was carried out for each spin state at the B3LYP/6-311G level,<sup>26</sup> and exchange couplings ( $J$  values) were obtained from a Heisenberg Hamiltonian ( $\hat{H} = -J S_1 \cdot S_2$ ) using the broken symmetry method of Noodleman.<sup>27,28</sup> The  $J$  value of the imidazolate intermediate was also obtained by performing geometry optimizations at the B3LYP/6-311+G(d) level (diffuse functions were not included on carbon), followed by application of the broken symmetry method.

## Results

The results of our calculations are highlighted in Table 1. There it can be seen that the imidazole complex is well described

(15) Loew, G. H.; Axe, F. U.; Collins, J. R.; Du, P. *Inorg. Chem.* **1991**, *30*, 2291-2294.

(16) Menyhard, D. K.; Naray-Szabo, G. *J. Phys. Chem. B* **1999**, *103*, 227-233.

(17) Wirstam, M.; Blomberg, M. R. A.; Siegbahn, P. E. M. *J. Am. Chem. Soc.* **1999**, *121*, 10178-10185.

(18) Edwards, S. L.; Raag, R.; Wariishi, H.; Gold, M. H.; Poulos, T. L. *P. Natl. Acad. Sci.* **1993**, *90*, 750-754.

(19) Schuller, D. J.; Ban, N.; van Huystee, R. B.; McPherson, A.; Poulos, T. L. *Structure* **1996**, *4*, 311-321.

(20) Kunishima, N.; Fukuyama, K.; Matsubara, H. *J. Mol. Biol.* **1994**, *235*, 331-344.

(21) Becke, A. D. *J. Chem. Phys.* **1993**, *98*, 5648-5652.

(22) Frisch, M. J.; Trucks, G. W.; Schlegel, H. B.; Gill, P. M. W.; Johnson, B. G.; Robb, M. A.; Cheeseman, J. R.; Keith, T.; Petersson, G. A.; Montgomery, J. A.; Raghavachari, K.; Al-Laham, M. A.; Zakrzewski, V. G.; Ortiz, J. V.; Foresman, J. B.; Cioslowski, J.; Stefanov, B. B.; Nanayakkara, A.; Challacombe, M.; Peng, C. Y.; Ayala, P. Y.; Chen, W.; Wong, M. W.; Andres, J. L.; Replogle, E. S.; Gomperts, R.; Martin, R. L.; Fox, D. J.; Binkley, J. S.; Defrees, D. J.; Baker, J.; Stewart, J. P.; Head-Gordon, M.; Gonzalez, C.; Pople, J. A. *Gaussian 94 (Revision E.2): Gaussian, Inc.: Pittsburgh, PA, 1995.*

(23) Bauschlicher, C. W. *Chem. Phys. Lett.* **1995**, *246*, 40-44.

(24) Chandrasekhar, J.; Andrade, J. G.; Schleyer, P. v. R. *J. Am. Chem. Soc.* **1981**, *103*, 5609-5612.

(25) Davidson, A. R.; Feller, D. *Chem. Rev.* **1986**, *86*, 681-696.

(26) In Gaussian 94 the 6-311G basis set includes the 6-311G basis for first-row atoms (Krishnan, R.; Binkley, J. S.; Seeger, R.; Pople, J. A. *J. Chem. Phys.* **1980**, *72*, 650-654), the McLean-Chandler (12s,9p) → (621111,52111) basis for second row atoms with the negative ion sets for P, S, and Cl (McLean, A. D.; Chandler, G. S. *J. Chem. Phys.* **1980**, *72*, 5639-5648), and the Wachters-Hay all electron basis set for the first transition row (Wachters, A. J. H. *J. Chem. Phys.* **1970**, *52*, 1033-1036; Hay, P. J. *J. Chem. Phys.* **1977**, *66*, 4377-4384), using the scaling factors of Raghavachari and Trucks (Raghavachari, K.; Trucks, G. W. *J. Chem. Phys.* **1989**, *91*, 1062-1065.)

(27) Noodleman, L. *J. Chem. Phys.* **1981**, *74*, 5737-5743.

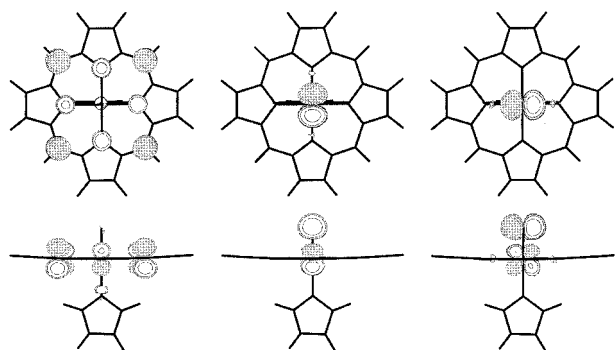


**Figure 1.** Natural orbitals of  $S = 3/2$  imidazole-ligated compound I intermediate with occupation numbers of 1.0. Top and side views are shown at a contour value of 0.05.

by the porphyrin radical cation model. The unpaired spin on its porphyrin and the  $S = 1$  iron-oxo unit couple ferromagnetically to give a quartet ground state. The strength of the spin coupling predicted at the B3LYP/6-311G level of theory ( $J = 99 \text{ cm}^{-1}$ ) is larger than that observed for model complexes, and stronger than that obtained by Kuramochi and co-workers, who calculated  $J = 1 \text{ cm}^{-1}$ .<sup>28</sup> Their value is in excellent agreement with that reported for HRP-I ( $|J| \leq 2 \text{ cm}^{-1}$ ), but seems fortuitous, as the same unoptimized structure was used to obtain the energies of both the quartet and doublet states.

The natural orbitals<sup>29–32</sup> (NOs) of the imidazole complex are shown in Figure 1. These NOs have occupation numbers of 1.00 (the rest are  $> 1.99$  or  $< 0.01$ ). Clearly these are the orbitals one would expect based on the porphyrin radical cation model. The two FeO  $\pi^*$  orbitals (center and right side of Figure 1) each contain one electron. These electrons couple ferromagnetically to give the well-characterized  $S = 1$  iron-oxo unit. The other natural orbital (left side of Figure 1) corresponds to the radical center. Assuming  $C_{2v}$  symmetry, the porphyrin-based radical transforms as  $A_1$ , while the orbitals of the FeO  $\pi^*$  set transform as  $B_1$  and  $B_2$ . As a result, the porphyrin-based radical has no overlap (zero overlap integral) with either of the iron-oxo  $\pi^*$  orbitals. This favors ferromagnetic coupling, resulting in an  $S = 3/2$  ground state.

Although porphyrin substituents and axial ligands can reduce the symmetry of synthetic model compounds to  $C_s$  or lower, experiments have shown that even in these systems the coupling remains ferromagnetic and similar to that found in perferryl species with more symmetrical substituents.<sup>9</sup> Thus, it appears that asymmetries, generated by axial ligands and ring substituents, do not contribute significantly to the antiferromagnetic component of  $J$  in perferryl species with porphyrin-based radicals, even though the orthogonality of the magnetic orbitals has been formally removed.

Figure 1 reveals the porphyrin spin density of the imidazole-ligated complex to have  $a_{2u}$  symmetry.<sup>33</sup> It has been suggested that non-meso porphyrin substituents (similar to those found in nature) could alter the symmetry of the radical species, changing

(28) Kuramochi, H.; Noodleman, L.; Case, D. A. *J. Am. Chem. Soc.* **1997**, *119*, 11442–11451.

(29) Natural orbitals are obtained by diagonalizing the SCF density matrix.

(30) Lowdin, P.-O. *Phys. Rev.* **1995**, *97*, 1474–1489.

(31) Szabo, A.; Ostlund, A. S. *Modern Quantum Chemistry: Introduction to Advanced Electronic Structure Theory*; Dover Publications: Mineola, New York, 1989.

(32) McWeeny, R. *Methods of Molecular Quantum Mechanics*; Academic Press: San Diego, CA, 1992.

(33) The porphyrin radicals of perferryl intermediates are generally discussed within the framework of  $D_{4h}$  symmetry, even though their symmetry may be lower.

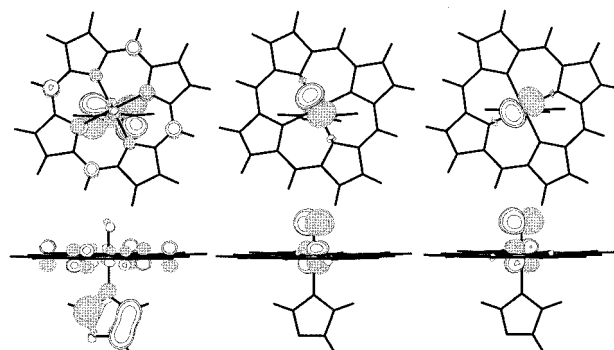


**Figure 2.** Natural orbitals of  $S = 3/2$  imidazolite-ligated compound I intermediate with occupation numbers of 1.0. Top and side views are shown at a contour value of 0.05.

it from  $a_{2u}$  to  $a_{1u}$ . When compared to an  $a_{2u}$  radical, an  $a_{1u}$  radical has spin density that is further removed from the  $S = 1$  iron-oxo unit.<sup>34</sup> As a result, weaker ferromagnetic coupling is expected for a compound I intermediate with an  $a_{1u}$  radical. Since the strongly coupled model systems are known to have radicals of  $a_{2u}$  symmetry, one possible explanation for the decreased  $J$  values of peroxidases is that the biological intermediates possess  $a_{1u}$  porphyrin radicals.

Fujii recently investigated this possibility by preparing a series of model complexes with  $a_{1u}$  porphyrin radicals.<sup>34,35</sup> As anticipated, the  $J$  values of these complexes fall within the range observed for peroxidases.<sup>8,36</sup> However, the NMR spectrum of Fujii's imidazole-ligated complex gives no indication that the radical species is delocalized to the axial ligand.<sup>37</sup> Thus, while the presence of an  $a_{1u}$  radical can explain the decreased  $J$  values observed for peroxidases, it cannot, at least by itself, account for the experimental findings of La Mar and co-workers.

Shown in Figure 2 are the NOs of the imidazolite complex with occupation numbers of 1.00 (the rest are  $> 1.99$  or  $< 0.01$ ). In contrast to the imidazole-ligated system, the imidazolite-ligated complex is not well described by the porphyrin-radical model. As can be seen in Table 1, the radical has a majority of its spin density (62%) on the axial ligand. This change in the location of the radical species results in a decrease in the magnitude of the spin coupling ( $J = 60 \text{ cm}^{-1}$  at the B3LYP/6-311G level of theory).

A thiolate-ligated compound I intermediate was also examined at the B3LYP/6-311G level. It, like the imidazolite complex, is not well described by the porphyrin-radical model. The thiolate axial-ligand possesses 81% of the radical's spin density. In agreement with experiment, the coupling for this species is predicted to be antiferromagnetic ( $J = -38 \text{ cm}^{-1}$ ).

Although the B3LYP/6-311G spin couplings calculated for our model systems show the proper trends, the couplings calculated for the imidazole/imidazolite systems are slightly larger than the experimentally determined values. To see if a smaller  $J$  value could be obtained, we reexamined the imidazolite-ligated species at a higher level of theory. Geometry optimizations were performed at the B3LYP/6-311+G(d)<sup>38</sup> level, followed by the application of Noodleman's broken symmetry method. Calculations at this level of theory result in increased ligand spin density (0.79) and a decrease in exchange

(34) Fujii, H. *J. Am. Chem. Soc.* **1993**, *115*, 4641–4648.

(35) Fujii, H.; Ichikawa, K. *Inorg. Chem.* **1992**, *31*, 1110–1112.

(36) Ayougou, K.; Mandon, D.; Fischer, J.; Weiss, R.; Muther, M.; Schunemann, V.; Trautwein, A. X.; Bill, E.; Terner, J.; Jayaraj, K.; Gold, A.; Austin, R. N. *Chem. Eur. J.* **1996**, *2*, 1159–1163.

(37) Fujii, H.; Yoshimura, T.; Kamada, H. *Inorg. Chem.* **1997**, *36*, 6142–6143.

(38) Diffuse functions were not included on carbon.

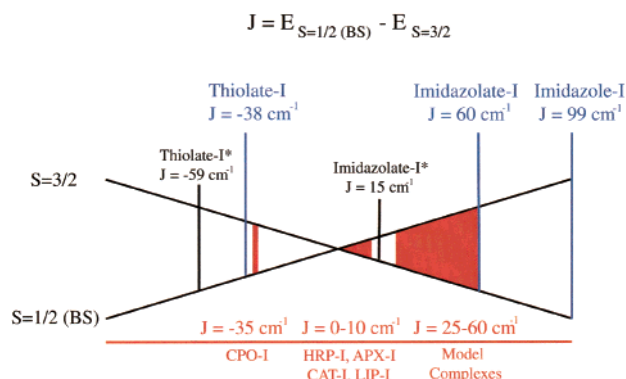


**Figure 3.** Experimental (red) and computational  $J$  values. The values shown in blue were obtained at the B3LYP/6-311G level of theory. The starred imidazolate/thiolate result (black) was calculated at the 6-311+G(d)/6-311+G level of theory. Diffuse functions were not included on carbon.

coupling ( $J = 15 \text{ cm}^{-1}$ ), in agreement with experiment (Figure 3). The thiolate-ligated system was also examined at a higher level of theory. Geometry optimizations at the B3LYP/6-311+G<sup>38</sup> level resulted in a slightly stronger antiferromagnetic coupling ( $J = -59 \text{ cm}^{-1}$ ), but no significant change in the ligand spin density (Table 1).

We initially used the geometries obtained at the B3LYP/6-311G level as input for single-point energy calculations at the B3LYP/6-311+G(d)<sup>38</sup> level. This common technique seemed to give results that were in excellent agreement with experiment. A coupling constant of  $J = -5 \text{ cm}^{-1}$  was obtained for the imidazolate-ligated complex, and  $J = 41 \text{ cm}^{-1}$  was predicted for the imidazole-ligated system. However, during the course of our investigation we determined that the use of this technique for the imidazolate-ligated complex was tenuous. We found that calculation of the B3LYP/6-311+G(d)<sup>38</sup> quartet at the B3LYP/6-311G optimized doublet geometry resulted in a quartet state that was lower in energy than the B3LYP/6-311+G(d)/B3LYP/6-311G<sup>38</sup> doublet. Thus, the imidazolate system was not actually antiferromagnetically coupled. Full optimization of the doublet and quartet states at the B3LYP/6-311+G(d)<sup>38</sup> level confirmed this, yielding  $J = 15 \text{ cm}^{-1}$ . As a result of this finding we have only presented data (Table 1) that were obtained by full geometry optimizations.

It is apparent from Table 1 and Figure 2 that delocalization of the radical onto the axial ligand affects the electronic coupling in two ways. First, increased spin density on the axial ligand necessarily results in decreased spin density on the porphyrin, which in turn results in smaller ferromagnetic contributions to  $J$ . Second, the symmetry character of the axial-ligand radical will generally not preclude it from having some overlap (nonzero overlap integral) with one of the members of the FeO  $\pi^*$  set. This overlap, unlike that generated by porphyrin asymmetry, does seem to contribute significantly to the antiferromagnetic component of  $J$  (e.g., consider the thiolate intermediate). Both of these factors will decrease  $J$  from the value found for a true porphyrin-radical.

The bond distances listed in Table 1 compare favorably with the available experimental data. An EXAFS study of horseradish peroxidase suggests an FeO bond length of  $1.64 \pm 0.03 \text{ \AA}$  and an average Fe–N distance of  $2.00 \pm 0.02 \text{ \AA}$ .<sup>39</sup> With the exception of the Fe–L bonds, the bond lengths listed in Table 1 are essentially the same for all three intermediates. At the

**Table 2.** Intraligand Bond Distances ( $\text{\AA}$ ) and Angles (deg) for Imidazole- and Imidazolate-Ligated Intermediates<sup>a,b</sup>

	bond distances			bond angles		
	imidazole I	imidazolate I	$\Delta^c$	imidazole I	imidazolate I	
N1–C2	1.40	1.36	–0.04	$\theta_{123}$	109.32	107.88
C2–C3	1.37	1.43	+0.06	$\theta_{234}$	105.81	109.52
C3–N4	1.39	1.36	–0.03	$\theta_{345}$	108.48	104.34
N4–C5	1.36	1.37	+0.01	$\theta_{451}$	109.87	113.47
C5–N1	1.34	1.39	+0.05	$\theta_{512}$	106.52	104.79

<sup>a</sup> The atom numbering scheme starts at the bound nitrogen in Figures 1 and 2 and continues clockwise. <sup>b</sup> Values listed are from geometry optimizations at the B3LYP/6-311G level. <sup>c</sup> Difference in bond lengths (imidazolate–imidazole).

6-311G level, the thiolate complex has an extremely long Fe–L distance of 2.79  $\text{\AA}$ , while the imidazole and imidazolate complexes have more normal bond lengths (2.13 and 2.11  $\text{\AA}$ , respectively). With the larger basis sets the Fe–L bond distances change by about 0.1  $\text{\AA}$ . The Fe–S bond shortens to 2.69  $\text{\AA}$ , while the Fe–N bond of the imidazolate intermediate lengthens to 2.19  $\text{\AA}$ . The long Fe–S bond length predicted for the thiolate compound I species shortens to 2.51  $\text{\AA}$  upon formation of compound II,<sup>40</sup> and can be understood in terms of the strong trans-influences of the oxo and thiolate ligands.<sup>41</sup>

The Mulliken spin densities obtained from the self-consistent field (SCF) calculations and the NOs are shown in Table 1. Using the singly occupied NOs to construct the spin density results in the removal of spin polarization effects. Thus, the NO spin densities shown in Table 1 (which are smaller than the SCF values) can be attributed solely to the unpaired electrons in the  $S = 1$  iron-oxo unit and the  $S = 1/2$  radical center. While the spin densities obtained for the imidazole complex agree with the values reported from other density functional calculations,<sup>28,42</sup> the values obtained for the imidazolate complex do not. Calculations by Deeth<sup>2</sup> predict a spin density of 0.21 on the imidazolate ligand, a value much smaller than the 0.79 we found.

In contrast to Deeth's, our calculations reveal significant differences between the structures of the axial-ligands in the imidazole- and imidazolate-ligated intermediates. These structural differences are directly linked to our prediction of an imidazolate-based radical. Optimization of the imidazolate-ligated intermediate's geometry was initiated using the structure of the imidazole-ligated species. At this geometry the  $S = 3/2$  imidazolate-ligated intermediate has a ligand spin density of 0.34, a value similar to Deeth's. However, as the structure of the imidazolate system was optimized (B3LYP/6-311G), this value grew to 0.60. Similar changes, although not as large, were observed when the B3LYP/6-311G geometry was used as input for optimizations at the B3LYP/6-311+G(d)<sup>38</sup> level. At this level of theory, the B3LYP/6-311G geometry has an imidazolate spin density of 0.68, while the optimized B3LYP/6-311+G(d)<sup>38</sup> structure has a ligand spin density of 0.79. These changes in spin density are accompanied by structural changes in the imidazolate ligand. Ligand bond lengths in the imidazolate-ligated intermediate differ by as much as 0.06  $\text{\AA}$  from those found in the imidazole-ligated complex (Table 2). The changes listed in Table 2 can be understood by examining the nodal pattern of the radical in Figure 2. Similar structural changes were observed in a density functional study of indolate radicals.

(40) Green, M. T. Unpublished.

(41) Ueyama, N.; Oku, H.; Kondo, M.; Okamura, T.; Yoshinaga, N.; Nakamura, A. *Inorg. Chem.* **1996**, *35*, 643–650.

(42) Antony, J.; Grodzicki, M.; Trautwein, A. X. *J. Phys. Chem. A* **1997**, *101*, 2692–2701.

(39) Penner-Hahn, J. E.; Eble, K. S.; McMurry, T. J.; Renner, M.; Balch, A. L.; Groves, J. T.; Dawson, J. H.; Hodgson, K. O. *J. Am. Chem. Soc.* **1986**, *108*, 7819–7825.

Walden and Wheeler found that bond lengths within the five-membered ring of indole change by as much as 0.07 Å upon formation of the indolate radical.<sup>43</sup>

Deeth's calculations suggest that the only significant difference between the geometries of the imidazole- and imidazolate-ligated intermediates is that the Fe–N<sub>imid</sub> bond is 0.04 Å longer in the imidazole-ligated system. That Deeth found no significant structural rearrangements within the imidazolate ligand is consistent with the fact that the method he used (SVWN5/ADFIV) predicts a porphyrin-based radical. Our results (see above) suggest that this prediction would not be modified by applying higher levels of theory to the SVWN5/ADFIV structure.

Thus, it appears that structural optimizations at the SVWN5/ADFIV level result in a porphyrin-based radical, while optimizations at the B3LYP/6-311+G(d)<sup>38</sup> level yield an imidazolate-based radical. The structure of the imidazolate ligand changes significantly when it is oxidized, and the amount of spin density possessed by the ligand is a function of these structural changes. Given that these two electronic structure methods predict different radical locations, a comparison with experiment is of interest. The methods employed in this paper predict structures and *J* values that agree with experiment. The SVWN5/ADFIV method employed by Deeth also predicts structures that agree with experiment. Deeth does not report *J* values.

## Conclusion

Our calculations strongly support experiments that suggest the Asp-His hydrogen bond of peroxidases modifies the electronic structure of compound I intermediates, by delocalizing the porphyrin radical onto the proximal histidine ligand. Radical

character on the axial ligand decreases the ferromagnetic and increases the antiferromagnetic contributions to *J*, resulting in reduced *J* values. The trends displayed at the B3LYP/6-311G level agree qualitatively with experiment, but the calculated couplings are slightly too large (Figure 3). Examination of the imidazolate-ligated species at the B3LYP/6-311+G<sup>38</sup> level yielded *J* = 15 cm<sup>-1</sup>, which is similar to the reduced couplings found in peroxidases. The bond distances calculated for the imidazole and imidazolate complexes are consistent with the values obtained from EXAFS experiments on HRP-I.

This report suggests that hydrogen bonds can modulate the electronic coupling between the radical species and the *S* = 1 iron-oxo unit. The proximal cysteinate ligands of chloroperoxidase and P450 accept hydrogen bonds from the protein matrix.<sup>44</sup> One might expect that the accepting nature of these hydrogen bonds would have an effect opposite to that observed for the histidine ligated systems. That is, these hydrogens bonds may make the thiolate axial ligand more difficult to oxidize. This would decrease the radical character on the proximal ligand, weakening the antiferromagnetic coupling. We are currently investigating this matter as well as the location of the radical species (and its effect on spin coupling) in the tyrosinate-ligated catalase compound I intermediate.

**Acknowledgment.** The author thanks Harry Gray, the Burroughs Wellcome Fund, and the National Institutes of Health for supporting this research.

JA994377K

(43) Walden, S. E.; Wheeler, R. A. *J. Chem. Soc., Perkin Trans. 2* **1996**, 2663–2672.

(44) Sundaramoorthy, M.; Ternier, J.; Poulos, T. L. *Structure* **1995**, *3*, 1367–1377.